Impedance and Noise of Passive and Active Dry EEG Electrodes: A Review

Erwin Habibzadeh Tonekabony Shad, Marta Molinas, *Member, IEEE*, and Trond Ytterdal, *Senior Member, IEEE*

***Abstract*—Dry electrodes are a promising solution for prolonged EEG signal acquisition, whereas wet electrodes may lose their signal quality in the same situation and require skin preparation for set-up. Here, we review the impedance and noise of passive and active dry EEG electrodes. In addition, we compare noise and input impedance of the EEG amplifiers. As there are multiple definitions of impedance in each EEG system, they are all first defined. Electrodes must be compatible with amplifiers to accurately record EEG signals. This implies that their impedance plays a significant role in amplifier compatibility and affects total input-referred noise. Therefore, we review the impedance and noise of state-of-the-art amplifiers and electrodes. Furthermore, we compare the various structures and materials used and their final impedance to that of wet electrodes. Finally, we compare state-of-the-art electrodes and amplifiers to the standards of the IFCN and IEC80601-2-26. We investigate bottlenecks and propose a guideline for future work on passive and active dry electrodes, as well as EEG amplifiers.**

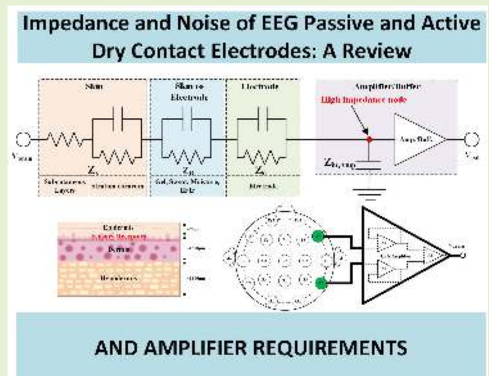

***Index Terms*— Electroencephalogram, dry electrode, active electrode, impedance, noise.**

I. Introduction

CURRENTLY, there are numerous techniques for monitoring brain activity, such as computer tomography (CT) [1], magnetic resonance imaging (MRI) [2], functional magnetic resonance imaging (fMRI) [3], positron emission tomography (PET) [4], magnetoencephalography (MEG) [5], and electroencephalogram (EEG) [6]. EEG signal acquisition is the least expensive and a suitable non-invasive technique for recording brain activity for applications such as brain computer interfaces (BCIs), due to its suitable temporal resolution. Furthermore, EEG techniques are comparably safe since the patient/user is not exposed to any strong external electrical or magnetic fields.

Manuscript received April 29, 2020; revised July 20, 2020; accepted July 20, 2020. Date of publication July 27, 2020; date of current version November 18, 2020. This work was supported by Enabling Technologies - NTNU, under the project “David versus Goliath: single-channel EEG unravels its power through adaptive signal analysis - FlexEEG”. The associate editor coordinating the review of this article and approving it for publication was Prof. Diego Barrettino. *(Corresponding author: Erwin Habibzadeh Tonekabony Shad.)*

Erwin Habibzadeh Tonekabony Shad and Marta Molinas are with the Faculty of Information Technology and Electrical Engineering, Engineering Cybernetics, Norwegian University of Science and Technology (NTNU), 7034 Trondheim, Norway (e-mail: erwin.shad@ntnu.no; marta.molinas@ntnu.no).

Trond Ytterdal is with the Faculty of Information Technology and Electrical Engineering, Department of Electronic Systems, Norwegian University of Science and Technology (NTNU), 7034 Trondheim, Norway (e-mail: trond.ytterdal@ntnu.no).

Digital Object Identifier 10.1109/JSEN.2020.3012394

Electroencephalography, or EEG, refers to the recording of electrical currents inside the brain through the scalp using metal or other conductive materials [7]. The electrical current is mostly due to the pumping of Na+, K+, Ca++, and Cl- ions through neurons. Due to rapid advancements in EEG technologies, the use of EEG systems is no longer limited to clinical applications, but is also now used for entertainment. It has been productively used in epilepsy, Parkinson’s disease, narcolepsy, depression, motor impairment, sports, entertainment, and computer-related functions [8]–[16].

In EEG, electrical activity of the brain is recorded through small flat metal discs, called electrodes, which are placed on the scalp. EEG-recording techniques, however, are not limited to electrodes on the scalp. For example, several studies have performed EEG on the ear [17], [18]. Furthermore, electrodes are not always metal and flat [19], [20], and a wide-variety of structures and techniques are used to capture EEG signals. Among the many existing ways to categorize electrodes, we divide them into two main sub-categories: wet electrodes and dry electrodes.

The most conventional clinical electrodes are wet electrodes. They utilize a saline or gel environment to increase the contact area, decrease impedance, and record high-quality signals. Although they exhibit minimum impedance and the best signal-to-noise ratio, they also have certain disadvantages. In general, the set-up time is relatively long for wet electrode EEG systems, a mess remains after use, and irritation results

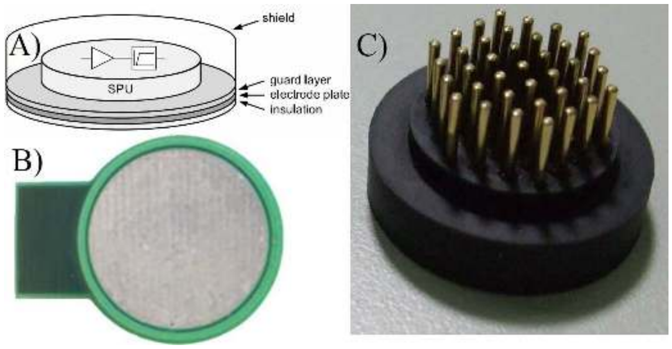

Fig. 1. Different types of dry electrodes: A) insulated electrode [22], B) non-contact electrode [23], and C) dry contact electrode [24].

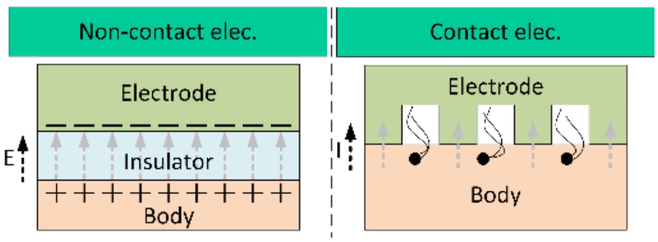

Fig. 2. Concept of contact and non-contact dry electrodes.

in some cases. One of the biggest problems, however, occurs when a signal needs to be recorded over a prolonged period of time. In this situation, signal quality decreases due to drying, which leads to the loss of signal. Body heat and air flow around a patient are two of the main sources that promote drying of the gel.

The second category consists of dry electrodes, which are more suitable for prolonged signal acquisition. A primary advantage of dry electrodes is that they do not require any special preparation. They are comprised of the following three sub-categories: contact electrodes, non-contact electrodes, and insulated electrodes. Although the terms non-contact and insulated electrodes might seem conceptually the same, they are practically different. The main difference between non-contact and insulated electrodes is that the bottom plate of insulated electrodes is an insulation material whereas the bottom plate of non-contact electrodes is made of metal and it couples through hair or clothing. The examples of contact, non-contact, and insulated electrodes are presented in Fig. 1. The concept of dry contact and non-contact electrodes are shown in figure 2. In dry contact electrodes, the current goes from body to electrode via contact area whereas non-contact electrodes work based on the electric field between body and electrode which are shown in figure 2. This electrical field can be modeled as a capacitor which constitute the basic concept of non-contact electrodes. The most important trade-off between all dry electrodes concerns user comfort and signal quality. Specifically, dry contact electrodes have a higher signal quality, but dry non-contact and insulated electrodes provide greater user comfort and easier set-up for applications that use one or two channels, such as those required in BCI. Moreover, although dry contact electrodes have a high offset, they also exhibit lower impedance than insulated and non-contact electrodes, and thus record EEG signals more accurately [21]. Fortunately, due to marked progress in circuit design, such a high offset is tolerable for their amplifiers. Consequently, we focus on dry contact electrodes due to their better signal quality and lower impedance.

A sweat bridge is created after prolonged use of either wet or dry electrodes [25]–[27]. This phenomenon is less common for non-contact dry electrodes. This artifact can be controlled for active dry electrodes by constant impedance monitoring at the point of contact and correcting the position of the electrode to minimize this effect.

Signal quality is derived from several parameters, of which noise and impedance are the two most important. Although the quality of the final signal is associated with the compatibility between the amplifier and electrodes, most of the exisiting literature has focused on electrodes instead of the entire system [28]–[30]. However, entire systems should be compared to find bottlenecks.

Here, we first attempt to define the different types of impedance in EEG systems, as there are several definitions, which may cause confusion. Then, we investigate different ways to reduce the impedance of dry electrodes by comparing various structures and materials. Subsequently, we introduce various noise sources and techniques to reduce them and investigate the noise and impedance of state-of-the-art amplifiers. Finally, we analyze the relationship between noise and impedance of the amplifier to identify bottlenecks in an EEG system.

II. Electrode Impedance and Its Importance for an Active Electrode

First, we need to examine two different categories of electrodes: passive electrodes and active electrodes. Although we have already categorized electrodes as either dry or wet, this further differentiation is necessary for a better understanding of the electrical behaviour of electrodes. An active electrode is a passive electrode with an inherent buffer or amplifier. We will discuss the necessity of using an amplifier or buffer inside an electrode after examining the properties of passive electrodes.

Electrodes exhibit different types of impedance. As depicted in Fig. 3, a simplified EEG amplifier and electrode can be modeled electrically with four types of impedance, in which three are related to the skin and electrodes and one is the input impedance of the amplifier, and an amplifier at the end. The offset of the electrode is eliminated from the electrical model to simplify it. The output of the amplifier in Fig 3 is not the output of an EEG amplifier. Practically, an EEG acquisition system can be as it's shown in Fig. 4 which is based on the structure in [31]. What is shown in Fig. 3 is up to the output of the amplifier $A1$ in Fig. 4.

Z_s is the skin impedance, which consists of several layers. The epidermis and dermis constitute the two top layers. The epidermis is the upper-most layer of the skin and exhibits the biggest impedance. The range of impedance of this skin layer varies from person to person, and is from approximately

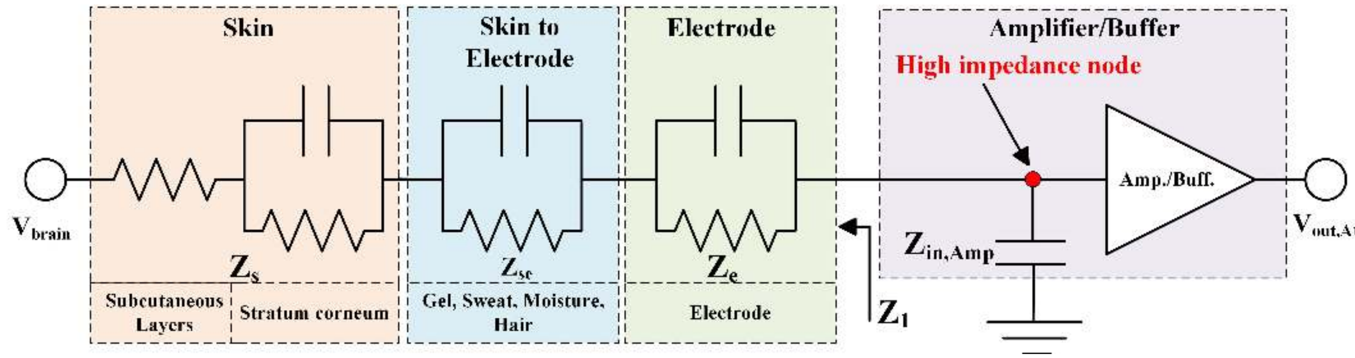

Fig. 3. Different types of impedance in a single dry electrode connected to an amplifier.

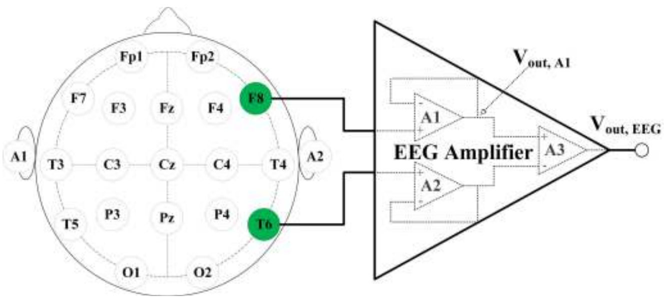

Fig. 4. EEG signal acquisition system.

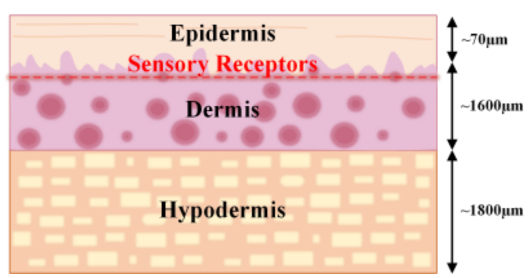

Fig. 5. The various layers of the scalp and their thickness.

10 kΩ to 1 MΩ per square centimeter at 1 Hz [32], [33]. The epidermis is comprised of two main layers: the stratum corneum and the stratum basale. The skin impedance can be equal to that of the upper-most layer, the stratum corneum, which is only $10-20$ μm thick [34]. Additionally, the thickness of the epidermis layer is approximately 70 μm and the total thickness of the scalp depends on the age of the person, but is approximately 3.4 mm for adults (Fig. 5) [35]. It is worth noting that the impedance of the dermis can be modeled by a single resistor. As the impedance of the other layers is frequency dependent, they should be modeled with at least one parallel capacitor and resistor. This means that the value of dermis impedance is constant at different frequencies, unlike that of the epidermis. The value for dermis impedance is approximately 100 Ω, which is considerably lower than that of the epidermis layer [36].

The second and most challenging type of impedance, after skin impedance, is the impedance between the skin and electrode, which is shown by Z_{se}. This type of impedance is the bottleneck in the design of dry electrodes. Its value varies according to the architecture, material, number of pins, and numerous other parameters. Wet electrodes have a lower impedance because of the gel or saline solution, which leads to an increase in the area of contact between the skin and electrode. The increased contact area leads to a reduced Z_{se} and the gel or saline environment leads to increased conductivity of the skin. In addition, the motions of the user cause this type of impedance to vary dramatically.

The third type of impedance is Z_e, which is related to the material, the amount of impurities, added substances, the shape and size of the electrode, and many other parameters. Fortunately this value is much smaller than other values in state-of-the-art dry and wet electrodes.

The final type of impedance concerns the input impedance of the amplifier, which is shown by $Z_{in,amp}$. Unlike other types of impedance, this value should be maximized to achieve minimum attenuation. The minimum acceptable value of this impedance is related to the aggregate value of the other types of impedance and acceptable attenuation. This value can thus be calculated according to equation (1), where Z_1 is calculated by equation (2), A is the gain of the amplifier, and is 1 for an ideal buffer. The measured value of electrode impedance on human skin is Z_1 for passive electrodes, whereas this value depends on the output impedance of the amplifier or buffer for active electrodes. Therefore, it can have a lower value.

$$V_{out} = A_v[\frac{Z_{in,amp}}{Z_{in,amp} + Z_1}]V_{brain} \tag{1}$$

$$Z_1 = Z_s + Z_{se} + Z_e \tag{2}$$

In the absence of other important factors, it would be possible to simply increase the $Z_{in,amp}$ and/or minimize the Z_1 to achieve minimum attenuation. Noise, however, constitutes another limitation in the design of electrodes. We will discuss the impact of noise after defining the noise equations. The typical value of $Z_{in,amp}$ is related to the technique used to reduce the noise of the amplifier, internal design, the technology used, and numerous other parameters. Chopping and auto-zeroing are the most conventional techniques [37], [38] currently used in most integrated biomedical amplifiers, especially integrated EEG amplifiers. The reported acceptable values of $Z_{in,amp}$ vary. According to the International Federation of Clinical Neurophysiology, the input impedance of an amplifier at 50/60 Hz should be greater than 100 MΩ [39] for wet electrodes. Dry electrodes usually have higher Z_1 than wet electrodes, and consequently they should have a higher $Z_{in,amp}$ for clinical applications.

Due to rapid advances in the field, the impedance of non-invasive dry contact electrodes is approximately limited to that of the upper-most layer of the skin, which is approximately 1 MΩ. This impedance is lower for invasive dry contact electrodes, as they penetrate the stratum corneum to make a low-impedance contact. In many cases, invasive dry contact electrodes have a similar, or even lower, impedance than do wet electrodes. Nevertheless, due to advances in dry contact electrodes, they are compatible with chopper amplifiers, with boosted input impedance, and insulated electrodes still exhibit high impedance in the EEG bandwidth. This is why circuit designers should utilize other techniques to use non-contact and insulated electrodes, as these electrodes have an approximate impedance above 1 GΩ at 1 Hz, whereas the nominal input impedance of EEG chopper amplifiers is only a few hundred mega-ohms.

When Z_1 is very high, high-impedance nodes behave like an antenna and absorb environmental noise, especially at 50/60 Hz. Designers thus employ inherent buffers to reduce the length of wiring nodes with high impedance. The buffer is used to take a signal with high impedance and transmit it at the same value, but with a lower impedance, at the cost of power consumption. In other words, they consume power solely to convert impedance [40]–[43]. In some cases, instead of using a buffer, circuit designers utilize amplifiers. As a result, they have not only an input signal with lower impedance at the output of the amplifier, but it is also of much higher amplitude. Consequently, they achieve a higher SNR, if the dominant noise doesn't come from the electrode itself. The first low-power active electrode application-specific integrated circuit (ASIC) system for EEG monitoring was designed in 2011 [44]. Although some active electrodes were already available, they used off-the-shelf components. Furthermore, a low output impedance amplifier helps to suppress cable artifacts and eliminate the need of using a shield for wires [45].

Overall, the performance of active electrodes is highly superior to that of passive dry electrodes, but at the expense of increased power consumption. ADS1299 is one of the conventional amplifiers used to implement an EEG amplifier and can also be used to measure the impedance of an electrode [46], [47].

III. Noise of Various Materials and Devices

Many different noise sources have been reported in the literature for wet and dry electrodes. Unfortunately, dry electrodes are more susceptible to noise due to their weak contact, which leads to higher impedance. Such high impedance is the consequence of the increment of Z_{se}, while Z_s and Z_e remain constant. Among the numerous sources, the most important are motion artifacts, thermal artifacts, flicker, line noise, and the half-cell effect at the skin-to- electrode interface [29], [48]. Generally, the accepted noise for electrodes is less than 2 μV_{rms} in the 1-100 Hz range when it is immersed in saline solution [49].

Thermal and flicker noise are two well-known noise sources in electrodes and/or amplifiers. Flicker noise, which is referred to as $1/f$ noise or pink noise, is dominant at lower frequencies. Although flicker noise is observed in most materials, the precise source is still unknown. Fortunately, the chopping technique helps to eliminate this noise in amplifiers with the help of modulation. The flicker-noise voltage power in a single MOSFETs (metal oxide semiconductor field effect transistors) is modeled as in equation (3) [50]:

$$V_{n,f}^2 = \frac{K}{C_{ox} W L f} \tag{3}$$

where W and L are the width and length of the channel of the MOSFET, respectively; C_{ox} the capacitor between gate and substrate; K the process-dependent constant; and f the frequency. Although this is the flicker noise of a single MOSFET, an increase in noise density can be observed at lower frequencies for a single small metal electrode or one of another material, proving the existence of flicker noise in other materials [29]. Finally, it is worth noting that bipolar and junction gate field-effect transistor (JFET) transistors have a lower flicker noise [51], [52]. As MOSFETs are much better for integration and the cost of production is less, circuit designers still use MOSFET, instead of bipolar or JFET transistors.

The thermal or white noise voltage power in a MOSFET gate can be calculated according to equation (4). In this equation, c is approximately 2/3 for a strong inversion bias, k is the Boltzmann constant, g_m the transconductance of the MOSFET, and T refers to room temperature in Kelvin. In addition, the thermal noise of a single resistor can be calculated according to equation (5), where R is the value of the resistor. Suppose that the impedance of a dry electrode is limited to the epidermis layer, which is approximately 1 MΩ. In this case, just the thermal noise of this tissue is 125 nV. If the desired EEG bandwidth is up to 200 Hz, the total input-referred noise will be approximately 1.7 μV_{rms} if this impedance is constant throughout this bandwidth. This would be just the thermal noise in this bandwidth, without any other noises of the electrode, if the electrode impedance on the skin is dominated by the resistance of the epidermis. However, if the contact between the electrode and skin is good, the capacitive behavior of the stratum corneum becomes dominant and the impedance value decreases as the frequency increases.

$$v_{nM,th}^2 = \frac{4kTc}{g_m} \tag{4}$$

$$v_{nR,th}^2 = 4kTR \tag{5}$$

A simplified electrical model for an active electrode with noise sources is depicted in Fig. 6. In this figure, Z_c is the active shield-to-electrode capacitance, and thus it can be modeled as a capacitor. Furthermore, v_n and i_n are the input-referred noise of the amplifier and the total current modulated noise in the node v_i, respectively. The total input-referred noise has two different sources: the thermal noise of the component and the noise of amplifier, as shown in equation 6. The effect of the noise of the amplifier can be calculated as in equation 7, whereas the input-referred thermal noise is calculated according to equation 8 at the input

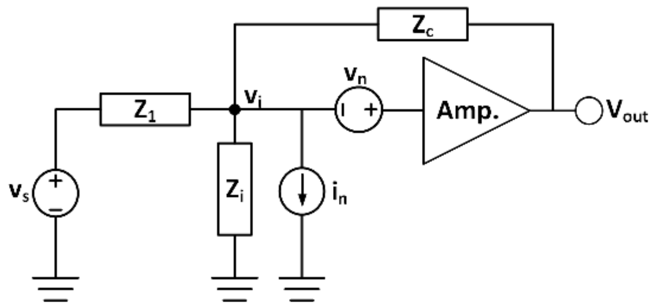

Fig. 6. Noise model for an EEG electrode system.

node [29].

$$v_{s,rms}^2 = v_{s,rms,1}^2 + v_{s,rms,2}^2 \tag{6}$$

$$v_{s,rms,1}^2 = \frac{(g_1 + g_i)^2 + \omega^2 (C_1 + C_i + C_c)^2}{g_1^2 + \omega^2 C_1^2} v_{i,rms}^2 \tag{7}$$

$$v_{s,rms,2}^2 = \frac{i_{i,rms}^2}{g_1^2 + \omega^2 C_1^2} = \frac{4kT}{g_1 + \frac{\omega^2 C_1^2}{g_1}} \tag{8}$$

where g is the conductance part of the admittance. If Z_1 of an electrode is low, the noise of the amplifier is approximately modeled at the input node without any increase. Otherwise, if Z_1 is high, e.g., an insulated electrode or a non-contact electrode, this noise will be modeled at the input node with a factor of $1 + (C_i + C_c)/C_1$.

It is important to note that the modeled thermal noise at an input node can be decreased by increasing and decreasing g_1, according to equation 8. Although it is mentioned in [29] that such thermal noise is dominated by skin-to-electrode impedance, due to tremendous progress in the design of dry electrodes, the dominant impedance is simply that of the stratum corneum as long as good contact is maintained between electrode and skin. However, if the contact becomes weak, the skin to electrode impedance becomes dominant, showing the importance of good contact between electrode and skin.

Another important type of noise consists of interface noise, e.g., 50/60 Hz noise. The electrical power line around electrodes is capacitively coupled to them [53]. Good shielding can reduce this contribution to noise. Active electrodes offer the best solution to reduce most noise sources, e.g., crosstalk, movement artifacts, noise pick-up, other forms of interference, and especially 50/60 Hz noise, due to its impedance conversion [54].

IV. Impedance Matching Approaches

According to equation (1), unlike electrodes, in which a reduction in impedance is desirable, an ideal amplifier should possess infinite input impedance. In the following subsections, we first review the existing approaches to decrease the impedance of dry electrodes, followed by a comparison of the impedance among them and finally a discussion of the input impedance of the suitable EEG amplifier.

A. Low-Impedance Dry Electrodes

EEG systems are broadly used and well-known due to their non-invasive approach to record brain signals. All clinical wet electrodes are non-invasive. Invasive dry electrodes just penetrate the stratum corneum, the upper-most layer of the skin, where there are no nerves to sense pain and where there is no bleeding. This is in stark contrast to the definition of conventional invasive approaches, in which some require removal of all the skin layers or even penetration of the skull. Moreover, as the quality of invasive and non-invasive approaches are not comparable, we categorize them into invasive and non-invasive dry electrodes below.

Wet electrodes, or wet Ag/AgCl, possess the best signal-to-noise ratio, whereas their main problem concerns gel dehydration over a prolonged time period. Thus, their impedance (Z_1) over a short period of time can serve as a good reference. Their normalized impedance is 114.9 ± 36.1 kΩ.cm^2 at 10 Hz [55]. At low frequencies, the impedance is approximately 34-37 kΩ, whereas this value drops to just 3.3-5.1 kΩ [56] at higher frequencies. The normalized Z_e for wet electrodes is approximately 1 kΩ.cm^2 and for a wet electrode with 333 mm^2 area [57], this impedance is less than approximately 300 Ω. The impedance of wet electrodes on skin is less than the epidermis impedance due to the different mechanism of EEG signal acquisition from wet electrodes. Specifically, they use conductive substances and hydrate the skin, and thus their impedance is smaller than that of the epidermis layer. Z_{se} of a dry Ag/AgCl on skin is 360 kΩ at 125 Hz [58]. As anticipated, dry Ag/AgCl has a relatively higher impedance than wet Ag/AgCl.

The shape of the electrode affects the contact area, which directly influences electrode impedance. Thus, each technique that increases the contact area will help to reduce impedance. This constitutes the biggest challenge in the design of low-impedance dry electrodes for hairy sites. In this case, hair increases impedance, which leads to significant attenuation of brain signals. Therefore, a low-impedance electrode for a hairy site should, at least, penetrate the hair to reach the skin. Furthermore, the amount of electrode pressure on the scalp can alter the measured impedance. In addition, high pressure may substantially decrease user comfort.

Several articles have reported normalized values of electrode impedance, in which the impedance was adjusted as a function of the area of the electrode. Although it would be best to compare the normalized impedance of each electrode, sufficient data in some articles are not available for such a comparison. Thus, we will focus on the reported data and then attempt to compare the reported values in Table I. The most important impedance in this table is Z_1 (as shown in Fig. 3), since it is comprised of all the types of impedance.

The g.SAHARASYS gold alloy coated electrode is amongst commercially available dry electrodes. This active electrode has eight tips of two different types, i.e., short and long tips of 7 and 16 mm in length, and is 19 mm in diameter. Their Z_{se} is 208 kΩ [58].

Drytrode is a well-known dry electrode from the Neuroelectrics company. It has 10 tips with a diameter of 1 mm. The total contact surface is 31 mm^2. The Z_e of this electrode is just below 2 kΩ at 10 Hz [57]. In most articles, the proposed electrode is usually compared to wet electrodes, Drytrode, or g.SAHARASYS as a reference electrode.

TABLE I
COMPARISON BETWEEN Z_1, Z_{se} AND Z_e OF VARIOUS TYPES OF ELECTRODES

	Non-invasive							Invasive			
Impedance	Wet Ag/AgCl	g.tech	[57]	[62]	[63]	[59]	[60]	[74]	[34]	[80]	[55]
Z_e	1 kΩ	-	4 kΩ	-	13 Ω	-	-	8 Ω	156 Ω	-	-
Z_{se}	35 kΩ	208 kΩ	-	300 kΩ	-	80 kΩ	10 kΩ	-	-	7-25 kΩ	-
Z_1	100 kΩ	1 MΩ* >	1 MΩ* >	1 MΩ* >	1 MΩ >	1 MΩ* >	1 MΩ* >	100 kΩ	-	-	87 kΩ

*expected values

We survey several dry electrodes in the following paragraphs. They were chosen based on their impedance values (Z_s, Z_{se} and Z_e), fundamental material, coating material, size, and shape. Their mechanical properties, for example stretchability and flexibility, are also investigated. Furthermore, several electrodes that can be fabricated by 3D printers are discussed because their mode of production makes them widely accessible.

1) Non-Invasive Dry Electrodes: The reverse-curve-arch-shaped dry electrode is one of the shapes proposed in [62]. It is made of sterling silver and a 3D printer was used in its manufacture. There are five arches of 10 mm^2, with a thickness of 2.5 mm. The Z_{se} of this electrode for hairy sites and bare skin are just below 300 kΩ and approximately 100 kΩ, respectively.

In [63], a flexible polymer-based dry electrode was produced for high user comfort. Moreover, 44% carbon was used to manufacture this active dry EEG electrode. The length, thickness, and density of the pins to penetrate hair are critical. Thus various structures were tested to find the best model. The final circular active EEG electrode is 5 mm in length and 13 mm in diameter. Despite all of these considerations, the final electrode has an impedance that is 10 times higher than that of conventional wet electrodes. The reported Z_1 of the electrode is 1 MΩ.cm^2 at 10 Hz, while its Z_e is approximately 10 Ω.cm^2.

In [57], a 3D-printed dry electrode was proposed with different length pins, to accommodate people with different hair densities. They did not report the Z_{se} in their paper, but their Z_e was comparable to that of wet electrodes. All of the samples showed an impedance of less than 4 kΩ at 10 Hz. Their experiments show that their electrodes could be used for BCIs, which do not require a high SNR.

Another type of dry electrode is the bristle dry electrode, proposed in [59]. They are comprised of a silver-coated polymer that is flexible, low-cost, and low-impedance, resulting in a passive electrode with 10 mm long bristles. Due to their long bristles, they can easily penetrate dense hairy sites and establish good contact with the skin. This helped them to achieve a Z_{se} of approximately 80 kΩ, while the dimension was 12 mm × 12 mm.

A dry electrode based on a conductive stretchable Ag nanowire/polydimethylsiloxane (NWs/PDMS) composite material has also been produced by 3D printing [60]. This dry electrode was utilized as an active electrode and achieves very good results in experiments on steady-state visual evoked potentials (SSVEP). The measured Z_{se} was approximately 10 kΩ at 10 Hz for F3 and Fp3 sites according to the international 10 - 20 system. In spite of its good performance on these sites, it is not a good choice for patients with dense hair, due to the absence of pins to penetrate hair, and this article contains no information about the dimension of the electrode.

Since moisture or water can reduce the impedance of the epidermis, a self-wetting paper electrode was proposed in [64]. The water content in the corneum acts as an electrolyte, as it contains ions, and helps to increase the effective contact area between the electrode and the skin. They used a porous fiber, which can absorb the moisture of the dermal layer. The porous fiber behaves like a reservoir when there is a barrier on top. This novel approach helped them to achieve a SNR similar to that of wet electrodes. EEG measurements while it was attached at the FP1 position showed the mean measured impedance to be 240 ± 51 kΩ, whereas the measured impedance for the wet electrode was 110 ± 52 kΩ. The size of the dry EEG electrode was not reported in the article. This electrode is not suitable for hairy sites, like other dry electrodes without bristles or pins. The Z_{se} of this electrode, after dropping a small amount of saline to wet the surface, was approximately 60 kΩ, and there were only negligible changes in this impedance during a 48-h experiment.

In [65], a dry polymer foam-based electrode for EEG measurements was introduced. It was made of an electrically conductive polymer foam covered with a conductive fabric. The electrode has the same Z_{se} impedance on the forehead and superior impedance at hairy sites. Moreover, skin preparation was not needed, whereas the reported wet electrode impedance in this article required skin preparation. The reported Z_{se} was approximately 10 kΩ on the forehead and 20 kΩ at 1 Hz. Furthermore, the proposed electrode is relatively inexpensive and was able to adapt to an irregular scalp surface.

Finally, many studies have tested coated pin-shape dry electrodes. However, a manufactured pin-shaped dry electrode may not possess good electrical properties. Consequently, the authors of these studies coated them with conductive materials, such as silver, tin, stainless steel, or gold-plated silver [66]. Although this technique may allow the production of inexpensive dry electrodes, they may lose their properties after long-term use. Thus, their performance must be checked regularly over the long term. Several examples of non-invasive dry electrodes are shown in Fig. 7.

2) Invasive Dry Electrodes: As previously discussed, the main bottleneck of high-impedance dry electrodes is related to the epidermis layers, especially the stratum corneum. Thus some research has focused on penetrating this layer with micro- or nano-needles, which results in a large reduction in measured impedance. Thus, they show higher signal quality than conventional dry electrodes, which absorb the signal from

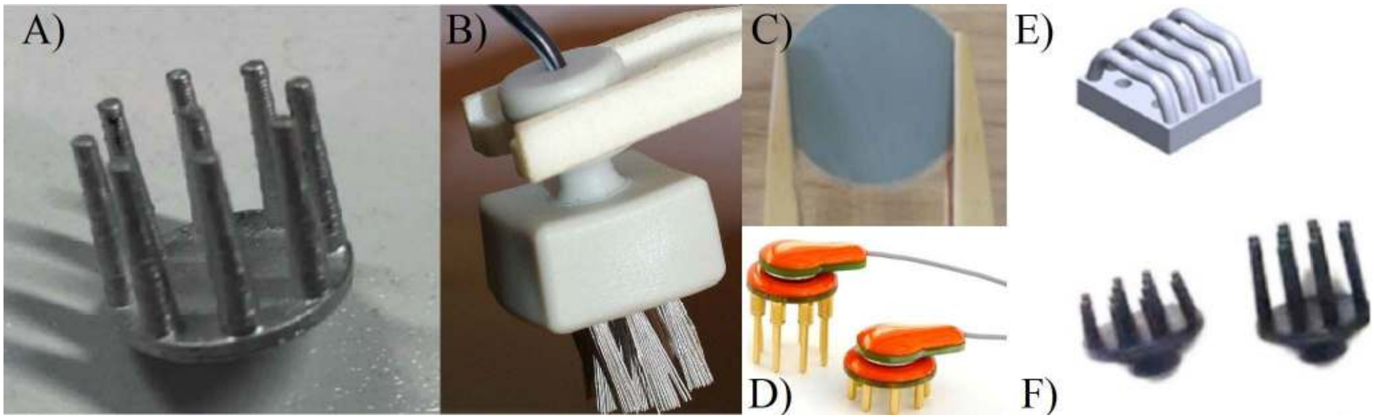

Fig. 7. Examples of non-invasive dry electrodes: A) 3D-printed electrode coated with silver paint [57], B) bristle dry electrode [59], C) Ag NWs/PDMS flexible dry electrode [60], D) g.SAHARASYS [61], E) reverse-curve-arch-shaped dry electrode [62], and F) micro-needle arrays dry electrode [63].

the top of the stratum corneum. Consequently, these electrodes perform much better, and are sometimes called non-invasive, as the user does not experience any pain. Nevertheless, they are somewhat invasive. Indeed, to avoid pain, the micro-needles should not reach the dermis. Thus, it is best that their penetration does not exceed 200 μm [67]. However, for reasons of safety, the penetration length should ideally be decreased to 70 μm, as the thickness of the epidermis layer reported in the medical literature is just 70 μm [35].

Micro-needle arrays (MNAs) show low impedance and good contact with the skin. They can be categorized into two major sub-categories. The first is stiff micro-needles, with a stiff substrate, such as silicon [63], titanium/titanium nitride [68], or brass [69]. They do not generally make a good contact with the skin, and thus need high pressure to achieve acceptable contact between the skin and the electrode. Thus, users will likely not feel comfortable during the experiment. The second sub-category consists of dry electrodes with flexible polymer micro-needles and substrate, such as polydimethylsiloxane (PDMS) [70] or SU-8 [71] to increase user comfort. However, although patients experience more comfort during the measurements, the skin-to-electrode impedance is higher, as their nonrigid micro-needles cannot easily penetrate the stratum corneum. Therefore, a dry electrode with stiff needles and a flexible substrate constitutes a good option.

After penetration into the skin, the material that is used on the outer layer of the electrode plays the most important role in the final impedance. Various materials have been investigated to identify the best quality of the recorded signal, including platinum, PEDOT/PSS [72], sintered Ag/AgCl, disposable Ag/AgCl, silver, gold-plated silver, stainless steel, tin [57], [66], and iridium oxide [34].

Multi-wall carbon nanotubes (MWCNTs), which have considerably higher conductivity, were used in [49]. Indeed, MWCNT of 10-15 μm in length have been used to penetrate the stratum corneum. Although the impedance of this electrode is not reported in the article, it is expected to be quite low.

A vertical patterned carbon nanotube was proposed in [73]. MWCNTs were grown vertically on a 2-mm thick stainless steel foil substrate. The height of each pillar was approximately 1-1.5 mm. The diameter of the circular substrate was 10 mm. The impedance of each pillar was approximately 7.5 kΩ at 40 Hz, while there were many pillars in each electrode. The final Z_e was less than 8 Ω. Its measured impedance (Z_1) on the skin was less than 100 kΩ, which is comparable to that of wet electrodes.

Several articles have reported that CNTs may be toxic in some cases. Furthermore, they cannot be grown beyond a certain height due to their mechanical properties. Consequently, they cannot sufficiently penetrate dense hair to make a good contact with the scalp. Given the high potential risk of CNTs, but their good properties, there is an extensive literature in this field that has focused on various parameters that affect the toxicity of CNTs, including size, length, agglomeration, and impurities [74]–[78].

In [34], a 100-200 μm tall micro-tip was used, which was coated with IrO to improve its contact with skin. The width of the micro-tip was 150-200 μm, which easily penetrates the stratum corneum. The dimensions of the square electrode were 8 mm $\times$ 8 mm. The Z_e of this electrode was approximately 100 Ω.cm^2. Moreover, it achieved the same performance as Ag/AgCl. However, below a frequency of 3 Hz, its electrode performance was more capacitive than Ag/AgCl.

In 2009, an innovative dry electrode was proposed that had micro-spike electrodes, consisting of a micro-pillar with a micro-tip on top. The micro-pillar was used to penetrate the hair, while the micro-tips were designed to penetrate the stratum corneum [79]. The final version of this dry electrode had a Z_{se} of 7-25 kΩ. In [67], the performance of an electrode with the same structure for hairy sites was tested and good results were achieved. In addition, they recorded EEG signals for open and closed eyes without any skin preparation or conductive gel. In 2018 [69], an ERP (event-related potential) was successfully recorded, which included P300, for unusual tasks from hairy sites.

A motion interference-insensitive flexible dry electrode was produced in [55]. It obtained a performance similar to that of wet electrodes, achieving a normalized impedance on skin half of that of wet electrodes. Its normalized Z_1 was 61.2 $\pm$ 31.3 Ω.cm^2 for a diameter of 1.2 cm.

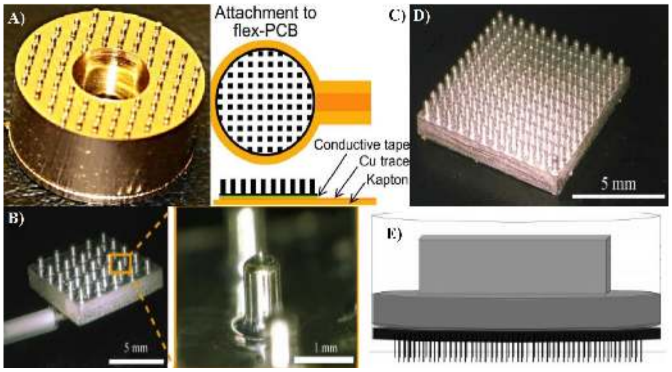

Fig. 8. Examples of invasive dry electrodes: A) micro-spike EEG electrode [79], B) candle-like dry micro-needle electrode [67], C) patterned vertical carbon nanotube electrode [73], D) newer version of candle-like dry micro-needle [67], and E) ENOBIO EEG electrode [49].

Various types of impedance of invasive and non-invasive dry electrodes are presented in Table I. The value of a wet Ag/AgCl electrode is reported to improve the comparison. Although the high impedance of dry electrodes is still a challenge, it can be compensated by high input impedance amplifiers. Therefore, we discuss high input impedance amplifiers in the next section.

B. High Input Impedance Amplifiers Suitable for Dry Electrodes

Most conventional amplifiers are not suitable for biomedical signals, particularly EEG signals, due to flicker noise of the amplifier at low frequencies. At such low frequencies, flicker noise is dominant, according to equation (3) and equation (4). This problem is more crucial when the designed circuit is going to be embedded at top of an electrode and the area is limited.

There are various types of low-noise amplifiers for biomedical applications. Most conventional EEG amplifiers use chopping techniques to eliminate flicker noise. Although this technique reduces flicker noise, it also decreases input impedance due to the parasitic capacitance of the input modulator, which is not desirable. Numerous techniques have been proposed to overcome this challenge, such as an auxiliary path [80], a positive feedback loop [81], bootstrap resistor [82], [83], or negative capacitor [84]. The input impedance of amplifiers using these techniques is compared in Table II. All of the devices used integrated circuits, and circuits with discrete elements can easily achieve superior specifications in noise and input impedance for clinical purposes at the cost of higher power and area consumption.

According to [39], the minimum acceptable input impedance for EEG amplifiers with wet electrodes is 100 MΩ. Typically, most state-of-the-art chopper amplifiers with boosted input impedance have an impedance of at least 100 MΩ, while their Z_1 is below 100 kΩ. Although this value is proposed for wet electrodes, these specifications could also be used for dry electrodes with the same skin impedance (Z_1). For electrodes with higher impedance, the amplifier should have higher input impedance to minimize attenuation.

TABLE II
INPUT-REFERRED NOISE AND INPUT IMPEDANCE OF EEG AMPLIFIERS

References	[86]	[87]	[88]	[81]
Year	2014	2015	2016	2016
Technology (nm CMOS)	180	180	180	40
Input impedance @50 Hz	400 MΩ	100 MΩ	6.7 GΩ	90 MΩ
Noise μV_{rms} (0.5 –100 Hz)	1.75	0.65	0.67	2

Finally, the input impedance of a differential amplifier with MOSFET transistors is much higher than these values, while they do not utilize chopping techniques. However, they have higher input-referred noise for the identical power and area consumption. For example, in [82], although the input-referred noise at lower frequencies is slightly higher, the input impedance is considerably higher than that of other devices, which is more than 50 TΩ.

V. NOISE REDUCTION APPROACHES

There are three main parts in each EEG system, each of which possesses its own ability to reduce noise. First, electrodes constitute the main contribution of noise and acquire the brain signal with unwanted noise. Secondly, amplifiers amplify the input signal and add additional unwanted noise to the EEG signal. Finally, signal processing extracts information from the EEG signal. Most existing techniques to reduce the noise in EEG signals have concentrated on signal processing. The goal of signal processing, of course, is to extract a clean signal. In the next two sections, we discuss techniques that are used at the level of the circuit or in electrodes to reduce noise.

A. Electrode Noise-Reduction Techniques

Most electrodes for hairy sites have various types of pins to penetrate through hair to achieve better contact with the skin, as well as a lower impedance. In addition, each electrode possesses a non-homogeneous nature of contact and there are variations in scalp surface due to sweat, hair density, and the shape of the skull [88]. All of these properties mean that the contact of each pin is different, with a different impedance, which results in a variable noise contribution.

In [89], configurable dry contact electrodes were studied, in which noisy pins were found and the corresponding signal is eliminated. Although most electrodes take the signal from all pins and send them from a single line, this study analyzed each first and then sent the low-noise signals to the next stage. Accordingly, they reduced noise from 3.6 μV to 2.1 μV. Thus, they reduced 40% of electrode noise at the expense of area, power consumption, and complexity.

Motion artifacts due to weak contacts between electrodes and skin present a major challenge. However, several solutions have been proposed to reduce this effect. The most conventional solutions use certain devices, such as EEG head caps, chin straps, or chest belts. It is therefore desirable that the designed electrodes be compatible with at least one of these motion-reduction devices.

Despite the use of such devices, weak contacts between electrodes and skin are still a problem. A low-impedance, skin-grabbing dry electrode was proposed in [90], [91] to solve this problem. In this technique, numerous micro-teeth are used to penetrate the epidermis to achieve a strong connection between electrode and skin. Through this approach, the electrode has comparatively lower sensitivity to motion artifacts.

As decreasing impedance leads to reducing input-referred noise, all techniques which reduce impedance will help to reduce noise in the electrode. The acceptable electrode impedance for EEG recording should be kept to less than 5 kΩ [39]. If we assume that the electrode impedance is 5 kΩ, then the Z_1 will be dominated by skin impedance when it is wet, and it is approximately 100 kΩ. Furthermore, the thermal noise will be 40 nV, according to equation (5). The total noise of such an electrode in the bandwidth of $0.5-100$ Hz is 400 nV. According to the measurements, flicker noise is dominant at lower frequencies, which leads to higher noise in the desired bandwidth. Therefore, in this bandwidth, the input-referred noise without calculation of the noise of the amplifier will be greater than 400 nV.

B. Amplifier Noise-Reduction Techniques

Although we have focused more on electrodes than amplifiers, the noise and input impedance of amplifiers play a significant role in the design of dry electrodes, while their input impedance can limit the performance of the electrode and their high noise may lead to loss of brain signal. Therefore, we discuss the required noise properties and those of state-of-the-art amplifiers in the following paragraphs.

The International Electrotechnical Commission (IEC) standared IEC80601 defines a series of technical standards for the safety and effectiveness of medical electrical equipment. According to the International Federation of Clinical Neurophysiology (IFCN), the total input-referred noise from 0.5 to 100 Hz should be less than 0.5 μV_{rms} or 1.5 μV_{pp} [39]. In addition, according to IEC80601-2-26, the input-referred noise per channel of an amplifier should be less than 6 μV_{pp} or 2.1 μV_{rms} in the bandwidth from 0.5 to 50 Hz [92].

The lowest noise can be achieved using the chopping technique with the same power and area consumption. According to Table II, most research has achieved noise lower than 2 μV_{rms} from 0.5 to 100 Hz. For example, in [93], the authors achieved 0.44 μV_{rms} from 0.5 to 250 Hz, while their input impedance was 1 GΩ at 60 Hz. Their total power consumption was 5.4 μW. Although most state-of-the-art amplifiers have slightly higher noise in the bandwidth of interest, according to IFCN standards, it is achievable with higher power consumption solely in the first stage amplifier if it limits the performance of the amplifier. Therefore, the bottleneck in designing an EEG amplifier suitable for dry electrodes is the input impedance of the amplifier.

Finally, important parameters of the amplifier are not limited to noise and input impedance. The common mode rejection ratio, power supply rejection ratio, tolerable offset, area consumption, and power consumption also affect the performance of an EEG system.

VI. Performance Comparison

Fundamentally, there is a trade-off between noise, user comfort, movement artifacts and sensor complexity. Generally, dry electrode signals show a slight amount signal degradation in comparison with wet electrodes and due to the weak contact, it's more susceptible to artefacts [94].

According to measurements, the noise of dry electrodes follows the equation 8 and they can be equal to wet electrodes [29]. Due to huge progress in dry electrodes technology, they comply with the needs of clinical EEG applications and higher user comfort is achieved for dry electrodes in comparison with wet electrodes [95]–[97]. This shows that most problems can be solved with careful circuit design [23].

Finally, for prolonged use, the signal quality of wet electrodes tend to degrade whereas the signal quality of dry electrodes will not degrade, and it even gets better for a period. As the skin under the electrode starts to sweat, the contact between electrode and skin will be improved [98]. This is good for long term recording whereas it's a disadvantage of dry electrodes in time constrained laboratory applications.

VII. Guideline to Reduce Noise and Impedance of Electrodes and Compatible Amplifiers

We have introduced various dry-electrode structures. Although pin-shaped and MNA dry electrodes are the most common structures for hairy sites, several flexible and flat electrodes have also been investigated due to their good impedance at other sites. Flat dry electrodes are not a good choice for use on hairy sites because of their weak contact with skin and their inability to penetrate hairy sites. Since the reference electrodes are generally used on the ear, flat dry electrodes can be utilized as a good reference.

There are many dry electrodes that are manufactured with 3D printers, offering the optimal solution for home-made electrodes in the near future. Thus, they could be a very inexpensive solution to manufacture the infrastructure. They can be coated with other materials to increase their conductivity or manufactured with 3D printers with conductive material at the cost of an increase in the price of the product.

Therefore, pin-shaped dry electrodes are the best choice for a non-invasive model. By contrast, MNA electrodes exhibit comparatively lower impedance, but they require special consideration, as they come into contact with skin and are intended to penetrate the first layer. A flexible substrate is preferable to maximize user comfort. In addition, the MNAs or pins should be sufficiently rigid to penetrate the stratum corneum and/or hair. By combining these structures, a low-impedance dry electrode with high user comfort can be achieved, making it suitable for long-term monitoring.

Until now, invasive dry electrodes have not been very popular because their impedance is generally limited by skin impedance. This highlights the pressing need for high input impedance amplifiers. We propose three EEG amplifiers that could be compatible with invasive, non-invasive, and insulated dry electrodes that comply with two international standards in Table III. Their features are based on electrode impedance on the skin of (Z_1), their sensitivity to power line noise, and their meeting international standards.

TABLE III
STANDARDS AND GUIDELINE TO DESIGN A COMPATIBLE AMPLIFIER FOR DRY ELECTRODES

Specs	IEC80601-2-26	IFCN	Proposed specification (for EEG amplifier)	Proposed specification (for EEG amplifier)	Proposed specification (for EEG amplifier)
Input voltage range	1 μV_{pp}	-	$> 1\ \mu V_{pp}$	$> 1\ \mu V_{pp}$	$> 1\ \mu V_{pp}$
Input-referred Noise (per channel)	6 μV_{pp} (0.5-50 Hz)	1.5 μV_{pp} 0.5 μV_{rms} (0.5-100 Hz)	1 μV_{rms} (0.5-100 Hz)	1 μV_{rms} (0.5-100 Hz)	1 μV_{rms} (0.5-100 Hz)
HPF cutoff frequency	<0.5 Hz	<0.16	<0.5 Hz	<0.5 Hz	-
Electrode offset tolerance	$\pm 150\ mV$	-	$\pm 150\ mV$	$\pm 150\ mV$	-
Input impedance (at 50/60 Hz)	-	> 100 MΩ	> 10 MΩ	> 100 MΩ	> 100 GΩ
CMRR (at 50/60 Hz)	> 80 dB	110 dB	> 80 dB	> 80 dB	> 80 dB
Power consumption (per channel)	-	-	4 μW	4 μW	10 μW
Application	Wet electrodes clinical	Wet electrodes clinical	invasive dry electrodes BCI	non-invasive dry electrodes BCI	Insulated dry electrode BCI
Impedance (Z_1) (at 1 Hz)	10 kΩ	<5 kΩ	100 kΩ	1 MΩ	1 GΩ

Although the amplitude of input signals is less than 1 mV_{pp}, artifacts may saturate the output and limit the performance of the amplifier. Therefore, a higher input range is proposed. Input referred noise is based on the required specification of the application. It can be a little higher or lower, depending on the sensitivity of the final application to noise. Since insulated electrodes are capacitively-coupled to amplifiers, there is no concern about the offset. Acceptable attenuation according to equation 1 defines the input impedance of the proposed amplifier. Power consumption is proposed according to that of state-of-the-art amplifiers.

A 0.05 Hz cut-off frequency leads to approximately a 20-s recovery time when there is an overload or artifacts [29]. Dry contact and non-contact electrodes have a weaker contact with skin than wet electrodes. Consequently, they are more susceptible to artifacts. As a result, a 0.5 Hz cut-off frequency is proposed. This frequency can be tuned according to the purpose of the application. If the signal below this frequency is important, this frequency should be reduced and then an additional circuit will be required to improve the recovery time.

The CMRR of an amplifier is equal to equation 9 where A_{dd} and A_{dc} are differential and common-mode gain of the amplifier [99]. The High impedance node behaves like an antenna and it absorbs environmental noise [21]. Although this problem can be mitigated by utilizing a low-output-impedance active electrode, if there is a mismatch between electrodes, this common-mode interference and motion artifact will be converted to a differential signal. Eventually, the amplitude of this signal may be much larger than that of the EEG signal. This problem is more critical when EEG recording and brain stimulation are performed simultaneously. In this case, the common-mode input signal may be up to 650 mV_{pp} [100]. In [101] The readers can find more information about CMRR and different sources for common mode signals reported in biomedical signals. As a rule of thumb, an amplifier with a high enough CMRR is essential to prevent output saturation. We propose a CMRR of 80 dB or more for BCI applications. For an amplifier with 40 dB differential gain, it means that it attenuates 600 mV common-mode signal to 6 mV which is acceptable value for most EEG applications.

$$CMRR = \frac{A_{dd}}{A_{dc}} = A_{dd}(dB) - A_{dc}(dB) \quad (9)$$

According to equation 8, the input-referred noise of insulated electrodes due to a very large g_1 is not dependent on C_1. Therefore, increasing C_1 simply decreases the impedance of the electrode (Z_1) and thus power-line noise will be reduced. In addition, a 100-GΩ input impedance amplifier using the chopping technique has not yet been reported. The proposed chopper amplifier in [100] has an input impedance of 1.6 GΩ at 20 Hz, which is among the highest reported with this structure, which is still much smaller than insulated electrodes. Therefore, an insulated dry electrode with smaller Z_1 is another way to fulfill the requirements. Thus, it would be compatible with chopping amplifiers, which leads to lower noise and substantially greater user comfort.

VIII. DISCUSSION

The performance of dry electrodes is not limited solely by their impedance and noise. Indeed, offset, drift, phase, cost of production, bio-compatibility, and user comfort must also receive serious consideration. In addition, one of the disadvantages of dry electrodes is their sensitivity to motion artifacts, especially if they have weak contact with skin. Although techniques which penetrate the stratum corneum may help to reduce this effect, it remains a major challenge in the progress of dry electrodes. EEG head caps have helped to decrease this effect, but they are not compatible with all dry electrodes and further development is necessary to ensure good contact at all sites. For example, electrodes do not make good contact with the scalp at the location of the visual cortex, even with a head cap. In spite of this potential shortcoming, compatibility of the designed electrode with head caps can still be a good feature to reduce motion artifacts.

IX. Conclusion

We have compared cutting-edge dry electrodes from the perspective of their impedance and noise. We also examined the compatibility of dry electrodes and amplifiers as an EEG system. Most integrated amplifiers have input impedance above 100 MΩ and lower than 2 μV_{rms} noise from 0.5 to 100 Hz. The most conventional electrodes are wet electrodes, which have an impedance below 100 kΩ on skin. Wet electrodes are however not a good choice for prolonged signal acquisition on wearable devices, for which dry electrodes are the optimal solution. However, their high impedance limits their performance in many cases. Various structures and materials have been proposed to decrease impedance (Z_1), which is currently limited to the upper-most layer of skin, the stratum corneum. This impedance is approximately 1 MΩ. However, we have presented several dry electrodes that have a similar impedance on skin as wet electrodes. We have also discussed various noise sources and ways to reduce input-referred noise and the noise contribution of electrodes and amplifiers. Motion artifacts due to the weak contact between electrode and skin remains one of the greatest challenges. Finally, we propose a guideline for the development of EEG systems. Although chopper amplifiers are widely used to minimize the noise of EEG amplifiers, they also decrease the input impedance, which is not desirable. We assessed the bottleneck in the design of an EEG system for dry contact electrodes by comparing state-of-the-art dry electrodes and amplifiers. Due to great progress in the design of dry contact electrodes, chopper amplifiers may become compatible with them through the use of input impedance boosting techniques. However, insulated electrodes are still not compatible with chopper amplifiers due to their high input impedance at very low frequencies.

Acknowledgment

The funder was not involved in the study design, collection, analysis, or interpretation of data, writing of this article, or the decision to submit it for publication.

References

[1] D. J. Brenner and E. J. Hall, "Computed tomography—An increasing source of radiation exposure," *New England J. Med.*, vol. 357, no. 22, pp. 2277–2284, 2007.

[2] M. L. G. Martín and P. L. Larrubia, Eds., *Preclinical MRI*. New York, NY, USA: Springer, 2018, doi: 10.1007/978-1-4939-7531-0.

[3] R. B. Buxton, *Introduction to Functional Magnetic Resonance Imaging*. Cambridge, U.K.: Cambridge Univ. Press, 2009, doi: 10.1017/cbo9780511605505.

[4] V. Kapoor, B. M. McCook, and F. S. Torok, "An introduction to PET-CT imaging," *RadioGraphics*, vol. 24, no. 2, pp. 523–543, Mar. 2004, doi: 10.1148/rg.242025724.

[5] P. Hansen, M. Kringelbach, and R. Salmelin, *MEG: An Introduction to Methods*. London, U.K.: Oxford Univ. Press, 2010.

[6] P. L. Nunez and R. Srinivasan, *Electric Fields of the Brain: The Neurophysics of EEG*. London, U.K.: Oxford Univ. Press, USA, 2006.

[7] E. Niedermeyer and F. L. da Silva, *Electroencephalography: Basic Principles, Clinical Applications, and Related Fields*. Philadelphia, PA, USA: Lippincott Williams & Wilkins, 2005.

[8] N. Verma, A. Shoeb, J. Bohorquez, J. Dawson, J. Guttag, and A. P. Chandrakasan, "A micro-power EEG acquisition SoC with integrated feature extraction processor for a chronic seizure detection system," *IEEE J. Solid-State Circuits*, vol. 45, no. 4, pp. 804–816, Apr. 2010.

[9] A.-T. Avestruz *et al.*, "A 5 μW/channel spectral analysis IC for chronic bidirectional brain–machine interfaces," *IEEE J. Solid-State Circuits*, vol. 43, no. 12, pp. 3006–3024, Dec. 2008.

[10] L. Nobili, A. Besset, F. Ferrillo, G. Rosadini, G. Schiavi, and M. Billiard, "Dynamics of slow wave activity in narcoleptic patients under bed rest conditions," *Electroencephalogr. Clin. Neurophysiol.*, vol. 95, no. 6, pp. 414–425, Dec. 1995. [Online]. Available: http://www.sciencedirect.com/science/article/pii/0013469495001387

[11] S. Debener, A. Beauducel, D. Nessler, B. Brocke, H. Heilemann, and J. Kayser, "Is resting anterior EEG alpha asymmetry a trait marker for depression?" *Neuropsychobiology*, vol. 41, no. 1, pp. 31–37, 2000. [Online]. Available: https://www.karger.com/DOI/10.1159/000026630

[12] B. Kamousi, Z. Liu, and B. He, "Classification of motor imagery tasks for brain-computer interface applications by means of two equivalent dipoles analysis," *IEEE Trans. Neural Syst. Rehabil. Eng.*, vol. 13, no. 2, pp. 166–171, Jun. 2005.

[13] E. Waterhouse, "New horizons in ambulatory electroencephalography," *IEEE Eng. Med. Biol. Mag.*, vol. 22, no. 3, pp. 74–80, May 2003.

[14] S. Park and S. Jayaraman, "Enhancing the quality of life through wearable technology," *IEEE Eng. Med. Biol. Mag.*, vol. 22, no. 3, pp. 41–48, May 2003.

[15] A. Casson, D. Yates, S. Smith, J. Duncan, and E. Rodriguez-Villegas, "Wearable electroencephalography," *IEEE Eng. Med. Biol. Mag.*, vol. 29, no. 3, pp. 44–56, May 2010.

[16] C.-T. Lin *et al.*, "Review of wireless and wearable electroencephalogram systems and brain-computer interfaces—A mini-review," *Gerontology*, vol. 56, no. 1, pp. 112–119, 2010. [Online]. Available: https://www.karger.com/DOI/10.1159/000230807

[17] P. Kidmose, D. Looney, M. Ungstrup, M. L. Rank, and D. P. Mandic, "A study of evoked potentials from ear-EEG," *IEEE Trans. Biomed. Eng.*, vol. 60, no. 10, pp. 2824–2830, Oct. 2013.

[18] V. Goverdovsky, D. Looney, P. Kidmose, and D. P. Mandic, "In-ear EEG from viscoelastic generic earpieces: Robust and unobtrusive 24/7 monitoring," *IEEE Sensors J.*, vol. 16, no. 1, pp. 271–277, Jan. 2016.

[19] Y.-J. Huang, C.-Y. Wu, A. M.-K. Wong, and B.-S. Lin, "Novel active comb-shaped dry electrode for EEG measurement in hairy site," *IEEE Trans. Biomed. Eng.*, vol. 62, no. 1, pp. 256–263, Jan. 2015.

[20] S. Lee, Y. Shin, S. Woo, K. Kim, and H.-N. Lee, "Dry electrode design and performance evaluation for EEG based BCI systems," in *Proc. Int. Winter Workshop Brain-Comput. Interface (BCI)*, Feb. 2013, pp. 52–53.

[21] J. Xu, R. F. Yazicioglu, C. V. Hoof, and K. Makinwa, *Low Power Active Electrode ICs for Wearable EEG Acquisition*. Cham, Switzerland: Springer, 2018, doi: 10.1007/978-3-319-74863-4.

[22] M. Oehler, P. Neumann, M. Becker, G. Curio, and M. Schilling, "Extraction of SSVEP signals of a capacitive EEG helmet for human machine interface," in *Proc. 30th Annu. Int. Conf. IEEE Eng. Med. Biol. Soc.*, Aug. 2008, pp. 4495–4498.

[23] Y. M. Chi, Y.-T. Wang, Y. Wang, C. Maier, T.-P. Jung, and G. Cauwenberghs, "Dry and noncontact eeg sensors for mobile brain–computer interfaces," *IEEE Trans. Neural Syst. Rehabil. Eng.*, vol. 20, no. 2, pp. 228–235, Dec. 2012.

[24] L.-D. Liao *et al.*, "A novel hybrid bioelectrode module for the zero-prep EEG measurements," in *Proc. IEEE Sensors*, Oct. 2009, pp. 939–942.

[25] W. O. Tatum, IV, *Atlas of Artifacts in Clinical Neurophysiology*. New York, NY, USA: Springer, 2018.

[26] P. M. R. Reis, F. Hebenstreit, F. Gabsteiger, V. von Tscharner, and M. Lochmann, "Methodological aspects of EEG and body dynamics measurements during motion," *Frontiers Hum. Neurosci.*, vol. 8, p. 156, Mar. 2014.

[27] A. M. Husain, *Practical Epilepsy*. New York, NY, USA: Springer, 2015.

[28] M. Lopez-Gordo, D. Sanchez-Morillo, and F. Valle, "Dry EEG electrodes," *Sensors*, vol. 14, no. 7, pp. 12847–12870, 2014.

[29] Y. M. Chi, T.-P. Jung, and G. Cauwenberghs, "Dry-contact and noncontact biopotential electrodes: Methodological review," *IEEE Rev. Biomed. Eng.*, vol. 3, pp. 106–119, 2010.

[30] C. Im and J.-M. Seo, "A review of electrodes for the electrical brain signal recording," *Biomed. Eng. Lett.*, vol. 6, no. 3, pp. 104–112, Aug. 2016.

[31] B. B. Winter and J. G. Webster, "Driven-right-leg circuit design," *IEEE Trans. Biomed. Eng.*, vol. BME-30, no. 1, pp. 62–66, Jan. 1983.

[32] J. Rosell, J. Colominas, P. Riu, R. Pallas-Areny, and J. G. Webster, "Skin impedance from 1 Hz to 1 MHz," *IEEE Trans. Biomed. Eng.*, vol. BME-35, no. 8, pp. 649–651, Aug. 1988.

[33] D. Prutchi and M. Norris, *Design and Development of Medical Electronic Instrumentation*. Hoboken, NJ, USA: Wiley, 2005.

[34] N. S. Dias, J. P. Carmo, A. F. da Silva, P. M. Mendes, and J. H. Correia, "New dry electrodes based on iridium oxide (IrO) for non-invasive biopotential recordings and stimulation," *Sens. Actuators A, Phys.*, vol. 164, nos. 1–2, pp. 28–34, Nov. 2010.

[35] H. Hori, G. Moretti, A. Rebora, and F. Crovato, "The thickness of human scalp: Normal and bald," *J. Investigative Dermatol.*, vol. 58, no. 6, pp. 396–399, Jun. 1972.

[36] B. A. Taheri, R. T. Knight, and R. L. Smith, "A dry electrode for EEG recording," *Electroencephalogr. Clin. Neurophysiol.*, vol. 90, no. 5, pp. 376–383, May 1994. [Online]. Available: http://www.sciencedirect.com/science/article/pii/0013469494900531

[37] Q. Fan, K. A. A. Makinwa, and J. H. Huijsing, *Capacitively-Coupled Chopper Amplifiers*. Cham, Switzerland: Springer, 2017, doi: 10.1007/978-3-319-47391-8.

[38] R. Wu, J. H. Huijsing, and K. A. A. Makinwa, *Precision Instrumentation Amplifiers and Read-Out Integrated Circuits*. New York, NY, USA: Springer, 2013, doi: 10.1007/978-1-4614-3731-4.

[39] M. R. Nuwer *et al.*, "IFCN standards for digital recording of clinical EEG," *Electroencephalogr. Clin. Neurophysiol.*, vol. 106, no. 3, pp. 259–261, Mar. 1998. [Online]. Available: http://www.sciencedirect.com/science/article/pii/S0013469497001065

[40] F. Z. Padmadinata, J. J. Veerhoek, G. J. A. van Dijk, and J. H. Huijsing, "Microelectronic skin electrode," *Sens. Actuators B, Chem.*, vol. 1, nos. 1–6, pp. 491–494, Jan. 1990. [Online]. Available: http://www.sciencedirect.com/science/article/pii/092540059080257Z

[41] S. Nishimura, Y. Tomita, and T. Horiuchi, "Clinical application of an active electrode using an operational amplifier," *IEEE Trans. Biomed. Eng.*, vol. 39, no. 10, pp. 1096–1099, Oct. 1992.

[42] T. Degen, S. Torrent, and H. Jackel, "Low-noise two-wired buffer electrodes for bioelectric amplifiers," *IEEE Trans. Biomed. Eng.*, vol. 54, no. 7, pp. 1328–1332, Jul. 2007.

[43] M. Fernandez and R. Pallas-Areny, "A simple active electrode for power line interference reduction in high resolution biopotential measurements," in *Proc. 18th Annu. Int. Conf. IEEE Eng. Med. Biol. Soc.*, vol. 1, Oct. 1996, pp. 97–98.

[44] J. Xu, R. F. Yazicioglu, B. Grundlehner, P. Harpe, K. A. A. Makinwa, and C. V. Hoof, "A 160 μw 8-channel active electrode system for EEG monitoring," *IEEE Trans. Biomed. Circuits Syst.*, vol. 5, no. 6, pp. 555–567, Dec. 2011.

[45] A. C. MettingVanRijn, A. P. Kuiper, T. E. Dankers, and C. A. Grimbergen, "Low-cost active electrode improves the resolution in biopotential recordings," in *Proc. 18th Annu. Int. Conf. IEEE Eng. Med. Biol. Soc.*, vol. 1, Oct. 1996, pp. 101–102.

[46] A. von Luhmann, H. Wabnitz, T. Sander, and K.-R. Müller, "M3BA: A mobile, modular, multimodal biosignal acquisition architecture for miniaturized EEG-NIRS-Based hybrid BCI and monitoring," *IEEE Trans. Biomed. Eng.*, vol. 64, no. 6, pp. 1199–1210, Jun. 2017.

[47] Y. Zou, V. Nathan, and R. Jafari, "Automatic identification of artifact-related independent components for artifact removal in EEG recordings," *IEEE J. Biomed. Health Informat.*, vol. 20, no. 1, pp. 73–81, Jan. 2016.

[48] E. Huigen, "Noise in biopotential recording using surface electrodes," Univ. Amsterdam Sect. Med. Phys., Amsterdam, The Netherlands, Tech. Rep., 2000.

[49] G. Ruffini *et al.*, "ENOBIO dry electrophysiology electrode; first human trial plus wireless electrode system," in *Proc. 29th Annu. Int. Conf. IEEE Eng. Med. Biol. Soc.*, Aug. 2007, pp. 6689–6693.

[50] B. Razavi, *Design of Analog CMOS Integrated Circuits*. New York, NY, USA: McGraw-Hill, 2005.

[51] A. J. Deen and O. Marinov, "Effect of forward and reverse substrate biasing on low-frequency noise in silicon PMOSFETs," *IEEE Trans. Electron Devices*, vol. 49, no. 3, pp. 409–413, Mar. 2002.

[52] F. A. Levinzon, "Measurement of low-frequency noise of modern low-noise junction field effect transistors," *IEEE Trans. Instrum. Meas.*, vol. 54, no. 6, pp. 2427–2432, Dec. 2005.

[53] A. Searle and L. Kirkup, "A direct comparison of wet, dry and insulating bioelectric recording electrodes," *Physiol. Meas.*, vol. 21, no. 2, p. 271, May 2000.

[54] C. M. Lopez *et al.*, "An implantable 455-active-electrode 52-channel CMOS neural probe," *IEEE J. Solid-State Circuits*, vol. 49, no. 1, pp. 248–261, Jan. 2014.

[55] H. Zhang *et al.*, "A motion interference-insensitive flexible dry electrode," *IEEE Trans. Biomed. Eng.*, vol. 63, no. 6, pp. 1136–1144, Jun. 2016.

[56] S. L. Kappel and P. Kidmose, "Study of impedance spectra for dry and wet EarEEG electrodes," in *Proc. 37th Annu. Int. Conf. IEEE Eng. Med. Biol. Soc. (EMBC)*, Aug. 2015, pp. 3161–3164.

[57] S. Krachunov and A. Casson, "3D printed dry EEG electrodes," *Sensors*, vol. 16, no. 10, p. 1635, Oct. 2016, doi: 10.3390/s16101635.

[58] Z. Zhao *et al.*, "Signal quality and electrode-skin impedance evaluation in the context of wearable electroencephalographic systems," in *Proc. 40th Annu. Int. Conf. IEEE Eng. Med. Biol. Soc. (EMBC)*, Jul. 2018, pp. 4965–4968.

[59] C. Grozea, C. D. Voinescu, and S. Fazli, "Bristle-sensors—Low-cost flexible passive dry EEG electrodes for neurofeedback and BCI applications," *J. Neural Eng.*, vol. 8, no. 2, Mar. 2011, Art. no. 025008, doi: 10.1088/1741-2560/8/2/025008.

[60] Z. Wang *et al.*, "A multichannel EEG acquisition system with novel ag NWs/PDMS flexible dry electrodes," in *Proc. 40th Annu. Int. Conf. IEEE Eng. Med. Biol. Soc. (EMBC)*, Jul. 2018, pp. 1299–1302.

[61] *g.tec Medical Engineering*. Accessed: Jul. 23, 2019. [Online]. Available: https://www.gtec.at

[62] J. S. Lee, K. S. Park, J. H. Kim, and C. M. Han, "Reverse-curve-arch-shaped dry EEG electrode for increased skin–electrode contact area on hairy scalps," *Electron. Lett.*, vol. 51, no. 21, pp. 1643–1645, Oct. 2015, doi: 10.1049/el.2015.1873.

[63] Y.-H. Chen *et al.*, "Soft, comfortable polymer dry electrodes for high quality ECG and EEG recording," *Sensors*, vol. 14, no. 12, pp. 23758–23780, Dec. 2014, doi: 10.3390/s141223758.

[64] X. Guo *et al.*, "A self-wetting paper electrode for ubiquitous bio-potential monitoring," *IEEE Sensors J.*, vol. 17, no. 9, pp. 2654–2661, May 2017.

[65] C.-T. Lin, L.-D. Liao, Y.-H. Liu, I.-J. Wang, B.-S. Lin, and J.-Y. Chang, "Novel dry polymer foam electrodes for long-term EEG measurement," *IEEE Trans. Biomed. Eng.*, vol. 58, no. 5, pp. 1200–1207, May 2011.

[66] P. Tallgren, S. Vanhatalo, K. Kaila, and J. Voipio, "Evaluation of commercially available electrodes and gels for recording of slow EEG potentials," *Clin. Neurophysiol.*, vol. 116, no. 4, pp. 799–806, Apr. 2005. [Online]. Available: http://www.sciencedirect.com/science/article/pii/S1388245704003906

[67] M. Arai, Y. Kudo, and N. Miki, "Electroencephalogram measurement from the hairy part of the scalp using polymer-based dry microneedle electrodes," in *Proc. 37th Annu. Int. Conf. IEEE Eng. Med. Biol. Soc. (EMBC)*, Aug. 2015, pp. 3165–3168.

[68] P. Fiedler *et al.*, "Multichannel EEG with novel Ti/TiN dry electrodes," *Sens. Actuators A, Phys.*, vol. 221, pp. 139–147, Jan. 2015. [Online]. Available: http://www.sciencedirect.com/science/article/pii/S0924424714004440

[69] Y. Yoshida, Y. Kudo, E. Hoshino, Y. Minagawa, and N. Miki, "Preparation-free measurement of event-related potential in oddball tasks from hairy parts using candle-like dry microneedle electrodes," in *Proc. 40th Annu. Int. Conf. IEEE Eng. Med. Biol. Soc. (EMBC)*, Jul. 2018, pp. 4685–4688.

[70] C.-Y. Chen, C.-L. Chang, T.-F. Chien, and C.-H. Luo, "Flexible PDMS electrode for one-point wearable wireless bio-potential acquisition," *Sens. Actuators A, Phys.*, vol. 203, pp. 20–28, Dec. 2013. [Online]. Available: http://www.sciencedirect.com/science/article/pii/S0924424713003944

[71] Y. Nishinaka, R. Jun, G. Prihandana, and N. Miki, "Fabrication of polymeric dry microneedle electrodes coated with nanoporous parylene," in *Proc. 17th Int. Conf. Solid-State Sensors, Actuat. Microsyst. (TRANSDUCERS & EUROSENSORS XXVII), Transducers & Eurosensors XXVII*, 2013, pp. 1326–1327.

[72] X. Crispin *et al.*, "The origin of the high conductivity of poly(3,4-ethylenedioxythiophene)–poly(styrenesulfonate) (PEDOT–PSS) plastic electrodes," *Chem. Mater.*, vol. 18, no. 18, pp. 4354–4360, Sep. 2006.

[73] M. J. Abu-Saude and B. I. Morshed, "Patterned vertical carbon nanotube dry electrodes for impedimetric sensing and stimulation," *IEEE Sensors J.*, vol. 15, no. 10, pp. 5851–5858, Oct. 2015.

[74] C.-W. Lam, J. T. James, R. McCluskey, S. Arepalli, and R. L. Hunter, "A review of carbon nanotube toxicity and assessment of potential occupational and environmental health risks," *Crit. Rev. Toxicol.*, vol. 36, no. 3, pp. 189–217, Jan. 2006.

[75] C. P. Firme and P. R. Bandaru, "Toxicity issues in the application of carbon nanotubes to biological systems," *Nanomed. Nanotechnol., Biol. Med.*, vol. 6, no. 2, pp. 245–256, Apr. 2010.

[76] W. Yang, P. Thordarson, J. J. Gooding, S. P. Ringer, and F. Braet, "Carbon nanotubes for biological and biomedical applications," *Nanotechnol.*, vol. 18, no. 41, 2007, Art. no. 412001.

[77] R. Alshehri, A. M. Ilyas, A. Hasan, A. Arnaout, F. Ahmed, and A. Memic, "Carbon nanotubes in biomedical applications: Factors, mechanisms, and remedies of toxicity: Miniperspective," *J. Med. Chem.*, vol. 59, no. 18, pp. 8149–8167, Sep. 2016.

[78] N. Saito *et al.*, "Safe clinical use of carbon nanotubes as innovative biomaterials," *Chem. Rev.*, vol. 114, no. 11, pp. 6040–6079, Jun. 2014.

[79] W. C. Ng *et al.*, "Micro-spike EEG electrode and the vacuum-casting technology for mass production," *J. Mater. Process. Technol.*, vol. 209, no. 9, pp. 4434–4438, May 2009. [Online]. Available: http://www.sciencedirect.com/science/article/pii/S092401360800770X

[80] H. Chandrakumar and D. Marković, "5.5 A 2 μW 40 mVpp linear-input-range chopper- stabilized bio-signal amplifier with boosted input impedance of 300 MO and electrode-offset filtering," in *IEEE Int. Solid-State Circuits Conf. (ISSCC) Dig. Tech. Papers*, Jan. 2016, pp. 96–97.

[81] Q. Fan, F. Sebastiano, J. H. Huijsing, and K. A. A. Makinwa, "A 1.8 μw 60 nv/$\sqrt{}$Hz capacitively-coupled chopper instrumentation amplifier in 65 nm CMOS for wireless sensor nodes," *IEEE J. Solid-State Circuits*, vol. 46, no. 7, pp. 1534–1543, Jul. 2011.

[82] Y. M. Chi, C. Maier, and G. Cauwenberghs, "Ultra-high input impedance, low noise integrated amplifier for noncontact biopotential sensing," *IEEE J. Emerg. Sel. Topics Circuits Syst.*, vol. 1, no. 4, pp. 526–535, Dec. 2011.

[83] C. Harland, T. Clark, and R. Prance, "Electric potential probes-new directions in the remote sensing of the human body," *Meas. Sci. Technol.*, vol. 13, no. 2, p. 163, 2001.

[84] M. Saad, M. El-Nozahi, and H. Ragai, "A chopper capacitive feedback instrumentation amplifier with input impedance boosting technique," in *Proc. IEEE 59th Int. Midwest Symp. Circuits Syst. (MWSCAS)*, Oct. 2016, pp. 1–4.

[85] J. Xu *et al.*, "A wearable 8-channel active-electrode EEG/ETI acquisition system for body area networks," *IEEE J. Solid-State Circuits*, vol. 49, no. 9, pp. 2005–2016, Sep. 2014.

[86] J. Xu, B. Busze, C. Van Hoof, K. A. A. Makinwa, and R. F. Yazicioglu, "A 15-channel digital active electrode system for multi-parameter biopotential measurement," *IEEE J. Solid-State Circuits*, vol. 50, no. 9, pp. 2090–2100, Sep. 2015.

[87] X. Zhou, Q. Li, S. Kilsgaard, F. Moradi, S. L. Kappel, and P. Kidmose, "A wearable ear-EEG recording system based on dry-contact active electrodes," in *Proc. IEEE Symp. VLSI Circuits (VLSI-Circuits)*, Jun. 2016, pp. 1–2.

[88] V. Nathan and R. Jafari, "Reducing the noise level of EEG signal acquisition through reconfiguration of dry contact electrodes," in *Proc. IEEE Biomed. Circuits Syst. Conf. (BioCAS)*, Oct. 2014, pp. 572–575.

[89] V. Nathan and R. Jafari, "Design principles and dynamic front end reconfiguration for low noise EEG acquisition with finger based dry electrodes," *IEEE Trans. Biomed. Circuits Syst.*, vol. 9, no. 5, pp. 631–640, Oct. 2015.

[90] M. Sun, W. Jia, W. Liang, and R. J. Sclabassi, "A low-impedance, skin-grabbing, and gel-free EEG electrode," in *Proc. Annu. Int. Conf. IEEE Eng. Med. Biol. Soc. (EMBC)*, Aug. 2012, pp. 1992–1995.

[91] B. Luan, W. Jia, P. D. Thirumala, J. Balzer, D. Gao, and M. Sun, "A feasibility study on a single-unit wireless EEG sensor," in *Proc. 12th Int. Conf. Signal Process. (ICSP)*, Oct. 2014, pp. 2282–2285, doi: 10.1109/icosp.2014.7015401.

[92] *Medical Electrical Equipment—Part 2-26: Particular Requirements for the Basic Safety and Essential Performance of Electroencephalographs*, Standard IEC 60601-2-26, May 2019.

[93] U. Ha, J. Lee, M. Kim, T. Roh, S. Choi, and H.-J. Yoo, "An EEG-NIRS multimodal SoC for accurate anesthesia depth monitoring," *IEEE J. Solid-State Circuits*, vol. 53, no. 6, pp. 1830–1843, Jun. 2018.

[94] Y.-H. Chen *et al.*, "Soft, comfortable polymer dry electrodes for high quality ECG and EEG recording," *Sensors*, vol. 14, no. 12, pp. 23758–23780, 2014.

[95] H. Hinrichs, M. Scholz, A. K. Baum, J. W. Y. Kam, R. T. Knight, and H.-J. Heinze, "Comparison between a wireless dry electrode EEG system with a conventional wired wet electrode EEG system for clinical applications," *Sci. Rep.*, vol. 10, no. 1, pp. 1–14, Dec. 2020.

[96] J. W. Y. Kam *et al.*, "Systematic comparison between a wireless EEG system with dry electrodes and a wired EEG system with wet electrodes," *NeuroImage*, vol. 184, pp. 119–129, Jan. 2019.

[97] Y.-H. Yu, S.-W. Lu, L.-D. Liao, and C.-T. Lin, "Design, fabrication, and experimental validation of novel flexible silicon-based dry sensors for electroencephalography signal measurements," *IEEE J. Transl. Eng. Health Med.*, vol. 2, pp. 1–7, 2014.

[98] T. Yamamoto and Y. Yamamoto, "Analysis for the change of skin impedance," *Med. Biol. Eng. Comput.*, vol. 15, no. 3, pp. 219–227, May 1977.

[99] W. M. C. Sansen, *Analog Design Essentials*. New York, NY, USA: Springer, 2006.

[100] H. Chandrakumar and D. Marković, "An 80-mVpp linear-input range, 1.6-$G\Omega$ input impedance, low-power chopper amplifier for closed-loop neural recording that is tolerant to 650-mVpp common-mode interference," *IEEE J. Solid-State Circuits*, vol. 52, no. 11, pp. 2811–2828, Nov. 2017.

[101] N. V. Thakor and J. G. Webster, "Ground-free ECG recording with two electrodes," *IEEE Trans. Biomed. Eng.*, vol. BME-27, no. 12, pp. 699–704, Dec. 1980.

Erwin Habibzadeh Tonekabony Shad received the B.Sc. degree in electrical engineering from Guilan University, Iran, in 2015, and the M.Sc. degree in analog integrated circuit design from the Iran University of Science and Technology in 2018. He has been working on biomedical amplifiers since receiving the M.Sc. degree. He is currently pursuing the Ph.D. degree with the Norwegian University of Science and Technology (NTNU). He is working on chopper amplifiers for EEG signal acquisition in a commercially available 0.18 μm CMOS technology. He is also a part of the David versus Goliath: FlexEEG project, which works on EEG applications with dry electrodes.

Marta Molinas (Member, IEEE) received the B.Sc. degree in electromechanical engineering from the National University of Asuncion, Asuncion, Paraguay, in 1992, the M.Sc. degree in information engineering from Ryukyu University, Nishihara, Japan, in 1997, and the Ph.D. degree in electrical engineering from the Tokyo Institute of Technology, Tokyo, Japan, in 2000. She was a Guest Researcher with the University of Padova, Italy, in 1998. From 2004 to 2007, she was a Postdoctoral Researcher with the Norwegian University of Science and Technology (NTNU), Trondheim, Norway, where she was a Professor with the Department of Electric Power Engineering, from 2008 to 2014. She is currently a Professor with the Department of Engineering Cybernetics, NTNU. Her research interests include stability of complex power electronics systems, harmonics, oscillatory phenomena, and nonstationary signals from humans and machines. She serves as an Editor of the IEEE JOURNAL OF EMERGING AND SELECTED TOPICS IN POWER ELECTRONICS and the IEEE TRANSACTIONS ON ENERGY CONVERSION. She is an Associate Editor of the IEEE TRANSACTIONS OF POWER ELECTRONICS and the IEEE TRANSACTIONS ON INDUSTRIAL ELECTRONICS.

Trond Ytterdal (Senior Member, IEEE) received the M.Sc. and Ph.D. degrees in electrical engineering from the Norwegian Institute of Technology in 1990 and 1995, respectively. He was employed as a Research Associate at the Department of Electrical Engineering, University of Virginia, from 1995 to 1996, and as a Research Scientist at the Electrical, Computer, and Systems Engineering Department, Rensselaer Polytechnic Institute, Troy, New York, from 1996 to 1997. From 1997 to 2001, he worked as a Senior ASIC Designer at Nordic Semiconductor, Trondheim, Norway. Since 2001, he has been on the Faculty of the Norwegian University of Science and Technology (NTNU), where he is a Professor with the Department of Electronics and Telecommunications. He present research interests include design of analog integrated circuits, behavioral modeling and simulation of mixed-signal systems, modeling of nanoscale transistors, and novel device structures for application in circuit simulators. He has authored or coauthored more than 200 scientific articles in international journals and conference proceedings. He is a coauthor of the books *Semiconductor Device Modeling for VLSI* (Prentice Hall, 1993), *Introduction to Device Modeling and Circuit Simulation* (Wiley, 1998), and *Device Modeling for Analog and RF CMOS Circuit Design* (Wiley, 2003), and has been a contributor to several other books published internationally. He is also a co-developer of the circuit simulator AIM-Spice. He is a member of the Norwegian Academy of Technological Sciences.